Single-Crystalline Porous Indium Phosphide as Anode Material for Li-Ion Batteries

M.-D. Gerngross, E. Quiroga-González, J. Carstensen and H. Föll

J. Electrochem. Soc. 2012, Volume 159, Issue 12, Pages A1941-A1948.
doi: 10.1149/2.037212jes

Journal of The Electrochemical Society, **159** (12) A1941-A1948 (2012)
0013-4651/2012/159(12)/A1941/8/$28.00 © The Electrochemical Society

Single-Crystalline Porous Indium Phosphide as Anode Material for Li-Ion Batteries

M.-D. Gerngross,*,z E. Quiroga-González, J. Carstensen, and H. Föll

Institute for Materials Science, Christian-Albrechts-University of Kiel, 24143 Kiel, Germany

This paper reports on the electrochemical and photo-(electro)chemical fabrication of a single-crystalline porous InP anode, and its performance in Li-ion batteries. This anode exhibits high capacity per area (∼63 mAh/cm^2). It consists only of the active material (InP) and a thin Au layer as a current collector. The maximum possible capacity of InP (∼800 mAh/g) is achieved, which is much higher than the capacity of commercial graphite anodes (∼350 mAh/g). The total anode capacity is freely scalable by adjusting the InP membrane thickness. The paper also shows the fabrication processes and a thorough battery characterization by cyclovoltammetry and battery cycling tests in half-cells.
 [DOI: 10.1149/2.037212jes]

Manuscript submitted July 12, 2012; revised manuscript received August 29, 2012. Published October 1, 2012.

Good candidates for anodes of next generation Li-ion batteries are phosphide compounds;[1] many of them exhibit good cyclability and capacities larger than the capacity of graphite, being the most commonly used anode. In principle, orthorhombic P alone exhibits a gravimetric capacity of around 2600 mAh/g,[2] one of the highest among the materials making alloys with Li,[2,3] but its synthesis is difficult. On the other hand, the synthesis of different metal-phosphide MP_y compounds is already well understood and they exhibit a low polarization due to their metallic character.[1]

The metal phosphides can react in two ways with Li, depending on their crystalline structure:[2] a) Insertion reaction (intercalation): The phosphides reacting in this way show a good battery performance for some charging/discharging cycles, but then they suffer from large capacity fading as their structure starts to collapse because the large volume expansion accompanying Li incorporation eventually pulverizes the material due to mechanical stress as it is seen e.g. for Si anodes.[4] b) Conversion reaction: It consists of a redox reaction of Li with just P or also with the metal (the metal could be a simple "spectator" or an active material, providing additional Li storage capacity). InP is a good example of a material where both components react with Li. For thin film anodes, the reaction can be expressed as:[5,6]

$$a\,\mathrm{InP} + b\,\mathrm{Li} \rightarrow c\,\mathrm{Li}_x\mathrm{In} + d\,\mathrm{Li}_y\mathrm{P}. \qquad [1]$$

State of the art InP anodes for Li-ion batteries are thin film anodes deposited by pulsed laser deposition[5] or in slurry form[6] with a stainless steel foil as substrate material. The big drawback of thin film anodes is the small energy density, since the active layer consists in maximum of several hundreds of nanometers. Nevertheless, this is highly beneficial for the diffusion of Li into the active anode layer resulting in a high power density. By using 3D structures as active material it is possible to increase the energy density of the anode while maintaining the high power density of thin film anodes.

Besides this, present InP anodes use stainless steel foils as substrate[5,6] and special binders,[6] which add substantial weight to the anode.

In this paper an approach will be discussed which has already been used in a similar way for Si to produce efficient anodes as follows. There is a number of reports on porous semiconductors (especially Si) where the porosity provides necessary space to - at least partially - compensate the volume expansion of the active material during lithiation, minimizing local stresses.[7–9] Thus, current-line-oriented pores (curro-pores) are etched in a single-crystalline InP wafer to generate enough space for the volume expansion due to lithiation and to achieve an extremely high surface area, and relatively thin walls, which can withstand the mechanical stress arising from the volume expansion. The electrolyte-filled pores allow an easier diffusion of Li ions into the InP, giving functionality to the thick anodes (they could be as thick as an InP wafer), which have a much higher capacity per area than the ones based on thin films. The anodes are membrane-like, not containing any bulk material that easily pulverizes upon cycling and adds "dead" weight to the anode. In this work we focus on the fabrication and electrochemical characterization of our new type of anode material for Li-ion batteries.

Experimental

In this work single-crystalline (100) InP wafers, doped with S at a doping concentration of 1.1×10^{17} cm^{-3} and a resistivity of 0.019 Ωcm, were used. The InP wafers were double-side polished and epi-ready. The InP wafer thickness was 400 μm ± 10 μm. The sample size was $A = 0.25$ cm^2 in all cases. The curro-pores were etched in an electrochemical double cell[10,11] with a 6 wt% aqueous HCl electrolyte at 20°C.

The first step is the formation of the curro-pore array from the front side with optimized etching conditions: A homogeneous nucleation of the curro-pores is obtained by applying a voltage pulse of 15 V for 1 s, followed by a constant anodic potential of 10 V for 40 min. To prevent confusion, the side of the wafer containing the long, parallel oriented curro-pores will always be called the front side, while the opposite side being opened in the second step to form the membrane will be called back side. Forcing a current for a long time through the InP wafer produces a thin InP oxide layer on the back side of the sample. This layer is removed by photochemical etching in the same cell and the same HCl-based electrolyte for 30 min.

The second step to form the InP anode is the membrane formation step, i.e. etching-off completely the non-etched bulk back side. For this a mesoporous crysto-pore layer is grown from the back side of the sample under galvanostatic conditions at a current density of 12 mA/cm^2 for 80 min. During this process, the sample is simultaneously illuminated with blue light from the back side. The blue light illumination (Enfis UNO Tag LED array blue with a mean wavelength of 470 nm) selectively etches the mesoporous layer. To obtain a homogeneous and flat membrane surface the photoelectrochemical dissolution is stopped (applying 0 mA/cm^2) 30 min before the illumination is switched off. As electrolyte a 6 wt% aqueous HCl solution at 20°C is used. The LED array is operated at a constant current of 200 mA resulting in a radiant flux density of roughly 300 mW/cm^2.

In the third step, the InP membrane is post-etched in an HF : HNO_3 : EtOH : HAc electrolyte in a concentration ratio of 3 : 8 : 15 : 24 under a cathodic potential of −0.5 V for 48 h to homogeneously reduce the mean pore wall width from about 220 nm to 160 nm over the complete pore length.[12]

In the fourth step, an Au layer of about 450 nm is sputter deposited on the extremely smooth front-side of the sample to form the current collector of the anode.

Standard battery cycling experiments were performed in the operational voltage regime of 0.15–1.85 V at a charging rate of *C*/10 (the lithiation or delithiation takes 10 hours) at room temperature. The lithiation/delithiation reaction was switched to a potentiostatic mode

*Electrochemical Society Student Member.
zE-mail: mdg@tf.uni-kiel.de

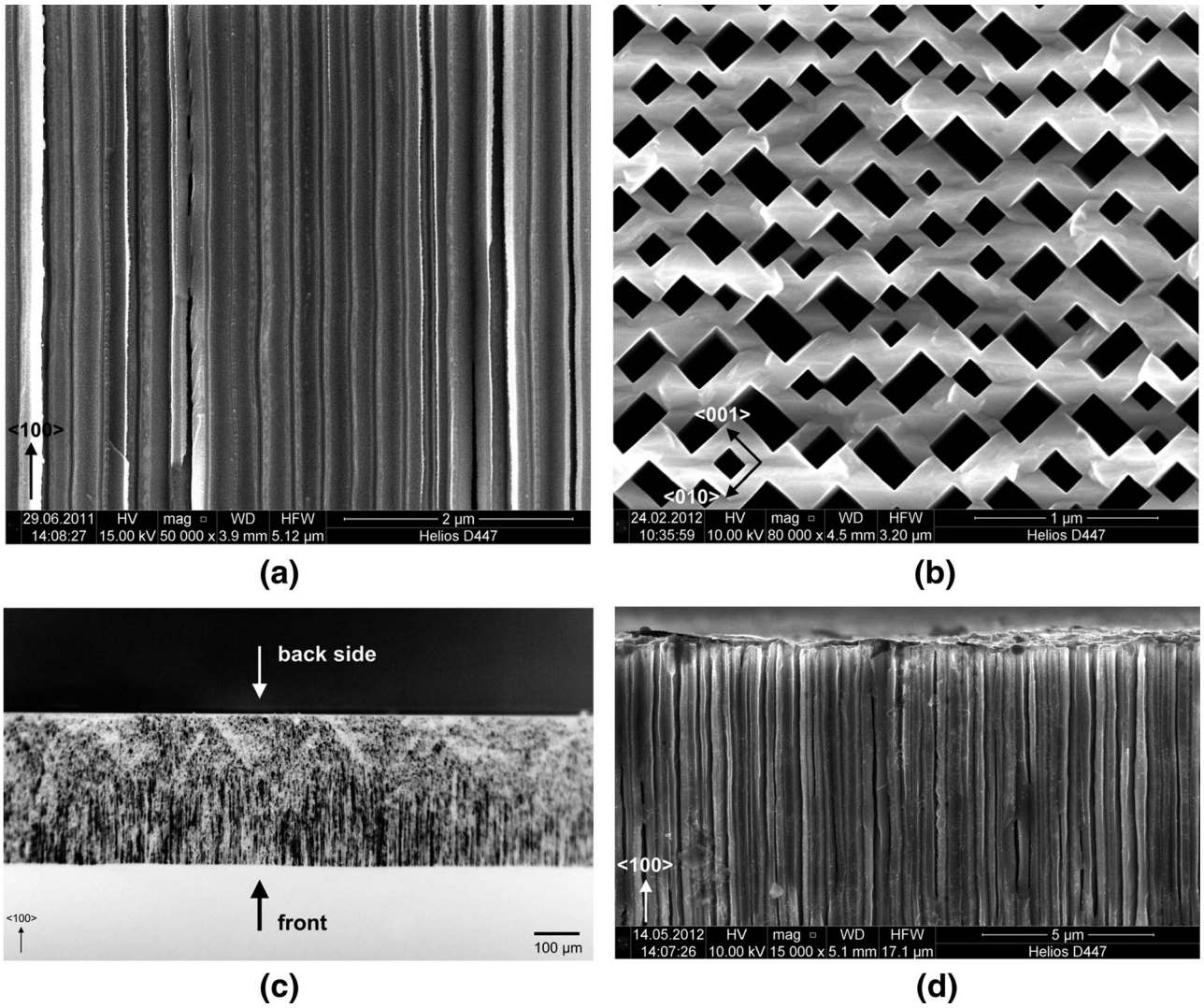

Figure 1. (a) Magnified cross-sectional view ((110) plane, vectors indicating pore orientation) on the InP pore structure, (b) top view on membrane back side ((100) plane, vectors indicating pore orientation) after post-etching, (c) cross-sectional image ((110) plane, vectors indicating pore orientation) of the complete InP membrane, and (d) cross-sectional view on the back side surface of the membrane ((110) plane, vectors indicating pore orientation).

when the voltage limits were reached; this mode is stopped as soon as the current declined to 10% of its original value, or if the capacity limit was reached. Just the first lithiation was allowed to the full capacity (800 mAh/g). The further cycling was performed to 80% of the full capacity.

Cyclic voltammetry tests were done with a scan rate of 0.1 mV/s in the range of 0 V to 2 V for 20 cycles. For both, the cycling tests and the voltammetry tests, half battery cells were prepared (using Li as counter electrode). The electrolyte was LP30 (0.5 ml), which consists of 1 mol/l of $LiPF_6$ salt in a 1 : 1 solution of ethylenecarbonate and dimethylcarbonate. The separator was a glass fiber microfilter from Whatman, with a pore diameter of 1 µm.

The structural characterization of the lithiated and delithiated porous InP anode was performed by means of XRD and SEM. A Seifert XRD 3000 TT tool was used for recording diffraction patterns using Cu K_α with a wavelength of 0.154 nm. The SEM investigation was performed with a Helios D477 SEM from FEI and an Ultra Plus SEM from ZEISS.

Results and Discussion

Anode fabrication.— In Fig. 1a and 1b the final pore structure after post-etching is depicted. The curropores have grown perfectly straight over the complete pore length. The pores are rectangular shaped, they show an almost equi-distant arrangement in an almost perfect hexagonally close packed structure. The mean pore wall width is about 160 nm. Figure 1c shows the cross-sectional image of the InP membrane after completing the membrane fabrication process. The membrane is thinned to a thickness of about 340 µm. This results in an anode aspect ratio of roughly 2,100. A magnified view of the membrane surface is depicted in cross-section in Fig. 1d showing the nicely opened back side of the membrane.

In Fig. 2 the completely processed InP anode is depicted. Fig. 2a shows the front side of the circular anode. It is completely covered with a 450 nm layer of Au for easy electric contacting. Figure 2b shows the back side of the anode, which is the active part of the anode. The anode is completely porous and freestanding with a very high mechanical stability, which makes handling easy. The surrounding bulk InP is completely removed, so that these anodes do not contain any non-porous parts, which might induce mechanical stress during cycling.

Cyclic voltammetry.— Figure 3 shows cyclic voltammetry curves of the InP anodes. In Fig. 3a two peaks positioned at 0.54 and 0.36 V are visible for the first negative voltage sweep (from larger to lower voltages). These peaks are related to the lithiation of InP. During

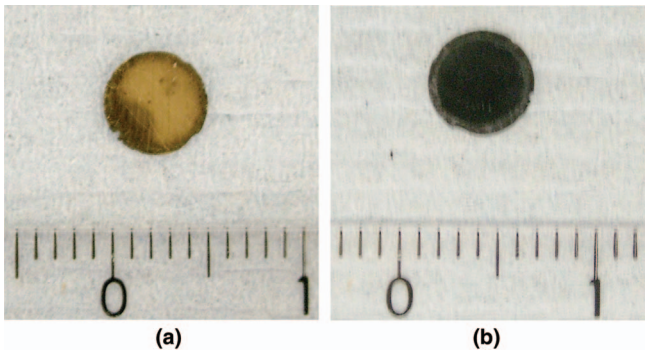

Figure 2. (a) Au contacted front side, and (b) open back side of the processed single-crystalline InP anode before first lithiation. The visible scale is 1 cm.

the first positive voltage sweep three peaks are found at 0.76, 0.92, and 1.3 V, respectively. These peaks are related to the delithiation process. In Fig. 3b clearly some of the peaks shift upon cycling. On the other hand, a new peak is found during the negative voltage sweeps at 0.9 V. During the positive voltage sweeps, a new peak at 1.7 V appears.

In X-ray diffraction (XRD) analysis of lithiated InP,[13] refraction peaks of Li_xIn alloys have been observed during the first negative sweep (below 0.25 V), and refraction peaks assigned to In have been observed during the first positive sweep at voltages above 0.67 V. On the other hand, in,[6] the battery cycling tests showed a long plateau

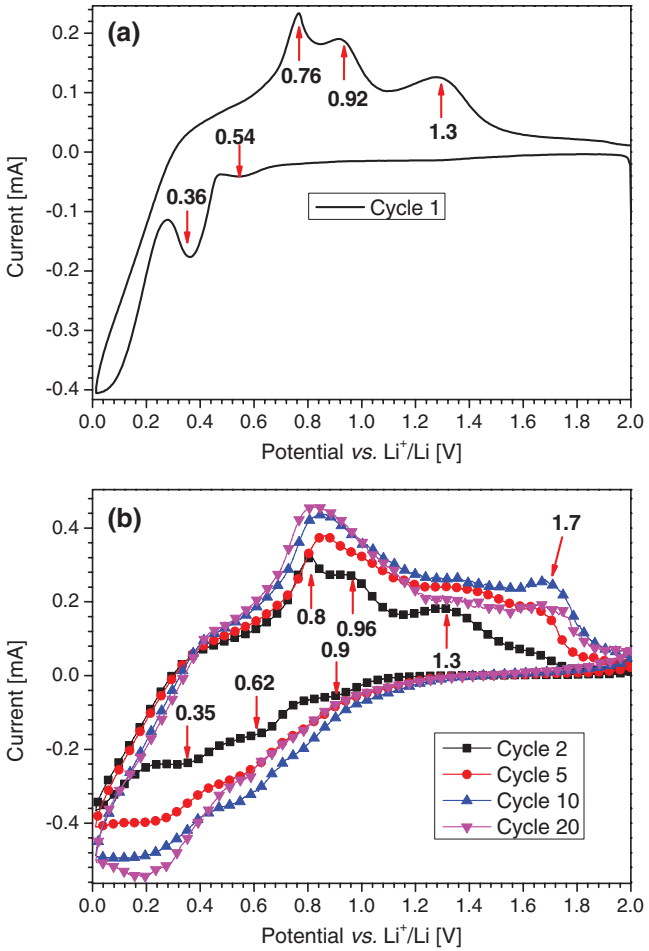

Figure 3. Cyclic voltammograms of the porous InP anode. (a) Data from first cycle; (b) data from selected cycles, starting from cycle 2.

at ∼0.3 V during lithiation, and a plateau at ∼0.75 V during the delithiation. Correspondingly in our electrodes the redox couple of ∼0.35 V and ∼0.8 V should be due to the formation of a Li_xIn phase, and the delithiation process to obtain In, respectively.

In the existing reports on InP anodes[5,6,13] a plateau at ∼1.5 V has been observed during the battery cycling tests, this being the maximum delithiation potential. The XRD investigation in[13] shows that when the InP anode is delithiated to a potential around 1.36 V, only the diffraction signals of InP are obtained. This is a good indication that the peak found at 1.3 V in the voltammogram during the positive sweep is due to the formation of InP.

No crystalline LiP phases could be identified by XRD in the existing reports on InP anodes,[5,6,13] either due to the particle size, or more probably because an amorphous phase has been formed. Nevertheless it was proven by X-ray photoelectron spectroscopy that a Li_3P alloy can be found in fully lithiated samples.[5] On the other hand, when lithiating black phosphorous (orthorhombic modification)[2] in the range of 0.6–0.8 V, a LiP phase could be identified by electron diffraction. Additionally, in voltammograms for the lithiation of Ni_2P, where Ni acts as a non-involved "spectator", a prominent peak was found at ∼0.6 V.[1] These observations lead to the assignation of the lithiation peak at ∼0.62 V to the formation of a Li_yP phase. Considering that the delithiation of P is a pre-requisite for the formation of InP (occurring at 1.3 V), the delithiation peak found for our samples at ∼0.96 V could be related with the delithiation of P. In fact, when delithiating Ni_2P, a peak at ∼1 V has been observed in voltammograms.[1] Therefore it is plausible to assume that the redox couple at ∼0.62 V and ∼0.96 V in our anodes is due to the formation of a Li_yP phase, and the delithiation of P, respectively.

In[6] the peak at ∼0.8 V appearing during the negative voltage sweep was assigned to the formation of a solid–electrolyte interface (SEI). As this peak (0.9 V in our anodes) is mainly observed in the first cycles (before the 5th cycle), the formation of an SEI is a very plausible explanation. Our battery cycling test results indicate that this process is not reversible. The existence of an SEI layer covering the walls of the InP membrane is evidenced with SEM micrographs, shown later in the paper.

During the first two cycles, below 0.25 V in the negative sweep, a fast decrease of the current is observed. This is a feature normally observed in anodes containing Au, mainly during the first cycles.[4,14] It has been discussed that Au could form an alloy with Li ($Li_{0.33}Au$) at low voltages and low sweep rates, but that this process is not reversible and kinetically limited.[4] This could explain why this feature is just observed during the first two cycles in our experiments.

The discharging peak at 1.7 V has not been observed before in InP anodes. A possible explanation for this peak is an alternative reaction for the formation of InP, which could be a single substitution of remaining LiP with In producing InP as a final product. This alternative reaction may be enabled due to mechanical stresses, which make the full delithiation process more difficult upon cycling (the voltammetric peak increases with the number of cycles).

From the voltammograms it could be also concluded that the operation range of the anode is between 0.15 and 1.85 V, which are the limits over which no more voltammetric events occur.

To corroborate our voltammetry findings, the anodes were also lithiated with constant current of *C*/10 until the potential reached 10 mV. The obtained voltage vs. capacity curve is shown in Fig. 4. As depicted, two plateaus at 0.33 and 0.17 V are easy to identify. Additionally the second derivative of the voltage vs. time (see inset in Fig. 4) was calculated in order to observe, at which points new formation reactions occur. In this curve, peaks at around 0.18, 0.34, and 0.66 V are observed, and are consistent with the position of the voltage plateaus in Fig. 4. The event at 0.17–0.18 V is in agreement with the estimated lower operation limit of the anode determined to be around 0.15 V by cyclic voltammetry. The other two events are at a position close to the lithiation peaks at ∼0.35 and ∼0.62 V, also observed in the voltammograms. This confirms the validity of the voltammetry observations, which were performed at slow rates to reach a quasi-static condition.

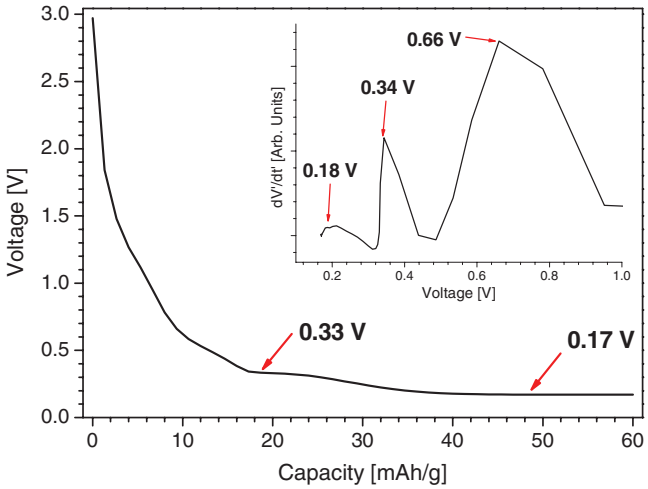

Figure 4. Voltage vs. capacity curve of the porous InP anode, lithiated at *C*/10. Two plateaus are easily identified. The inset of the figure shows the second derivative of the voltage with time; in this case peaks at 0.18, 0.34, and 0.66 V are observed, and could be attributed to start or end potential points of the lithiation processes.

Battery cycling tests.— There is a small controversy about the maximum possible capacity of InP. Values in the literature range from 780 mAh/g[5] to ∼1100 mA/g.[6,13] From the lithiation experiment at a constant voltage of 0.15 V (see Fig. 5) it was estimated that the capacity of our membrane anodes is around 800 mAh/g.

From Fig. 6a it can be observed that this maximum capacity is reached in the first cycle, and then a stable capacity of 640 mAh/g (the maximum capacity in the cycling program was set to 80% of the maximum capacity) is obtained in the following 6 cycles. After this point, there is a strong fading, probably caused by stress-induced degradation. From Fig. 6b it can be observed that the irreversible losses (capacity after lithiation – capacity after delithiation) and the fading (difference between contiguous cycles) have the same trend after the 6th cycle. This indicates that the irreversible losses occurring after the 6th cycle are the principal reason for the fading. These irreversible losses may be due to stress-induced detaching of material from the anode during cycling. This constant loss could be attributed to leakage currents (ohmic losses). Before the 6th cycle the irreversible losses could be mainly due to the formation of an SEI layer; this process is not reversible then. This result matches well with the interpretation of the voltammetric analyzes.

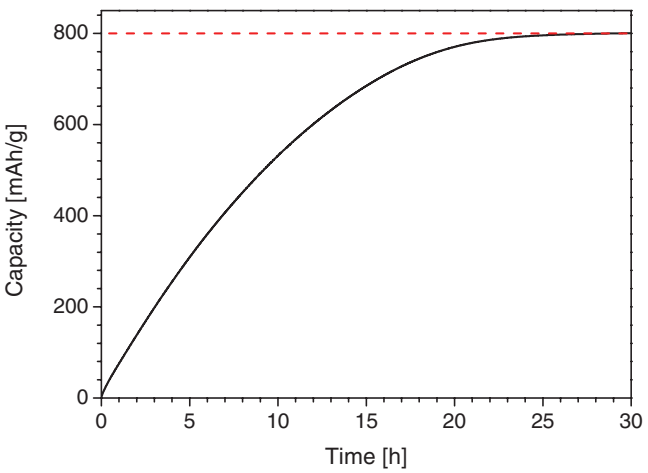

Figure 5. Charge vs. time curve of the InP anode when lithiated at a constant voltage of 0.15 V.

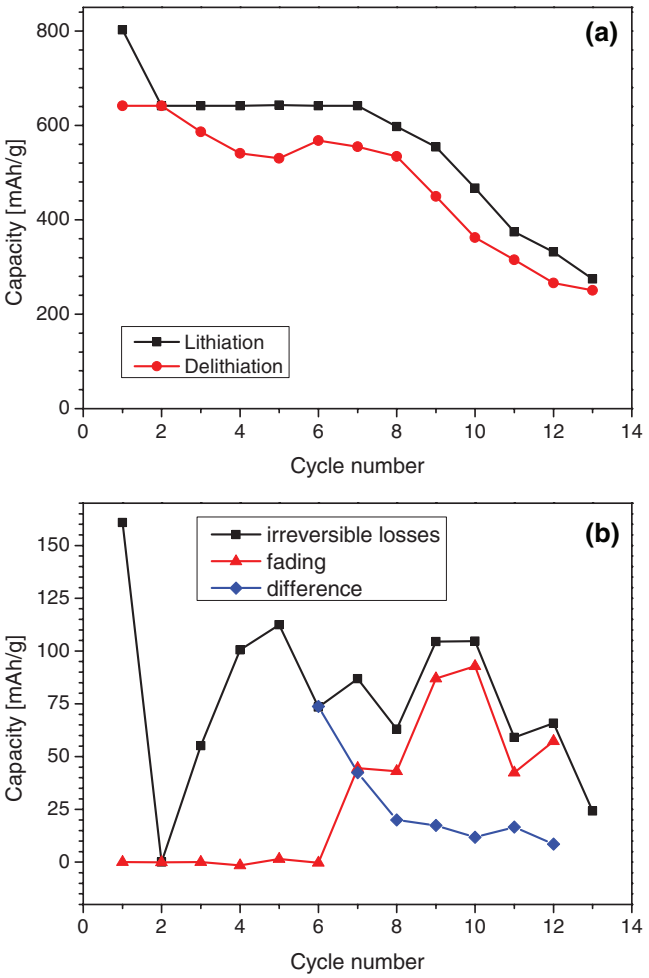

Figure 6. (a) Battery lithiation/delithiation cycling test on the InP anode at *C*/10 rate. Just the first lithiation was done to 100% of the maximum possible capacity (∼800 mAh/g), the further cycling was done to 80% (640 mAh/g). (b) Plot of irreversible losses and fading. The difference between these two parameters becomes constant and small upon cycling.

The cycling stability of anodes is highly affected by the cycling rate. The faster the charging and discharging of the anode is performed the lower is the cycling stability. The InP anode made by Satya Kishore is cycled at a rate of *C*/5 operated in the voltage range from 0.2–1.5 V showing a capacity fading of 67% of the initial capacity.[6] The trend in the fading of the gravimetric capacity is similar to what is observed for the porous InP anode presented in this paper. However the fading of the porous InP anode is just 42% of the initial capacity after 10 cycles indicating a higher cycling stability compared to the thin film anode made by Satya Kishore.

The cycling performance of Cui's InP anode is extremely good.[5] The fading of the anode is around 42% after 30 cycles. This excellent cycling stability can be explained by the extremely low charging rate / discharging rate related to the used current density of 10 $\mu A/cm^2$. This is about a factor 1600 smaller compared to the charging rate (*C*/10) used for the porous InP anode presented in this paper. Looking at the peak of the stainless steel substrate in the XRD patterns of the InP anode presented by Cui in,[5] a broadening and a right-shift of the stainless steal peak is clearly visible. This indicates that the stainless steel substrate also takes part in the lithiation and delithiation and hence affects the gravimetric capacity and cycling stability of the anode. Aditionally, the gravimetric capacity presented there is just the gravimetric capacity of the InP thin film, not taking into account the weight of the stainless steel substrate, which is also part of the anode.

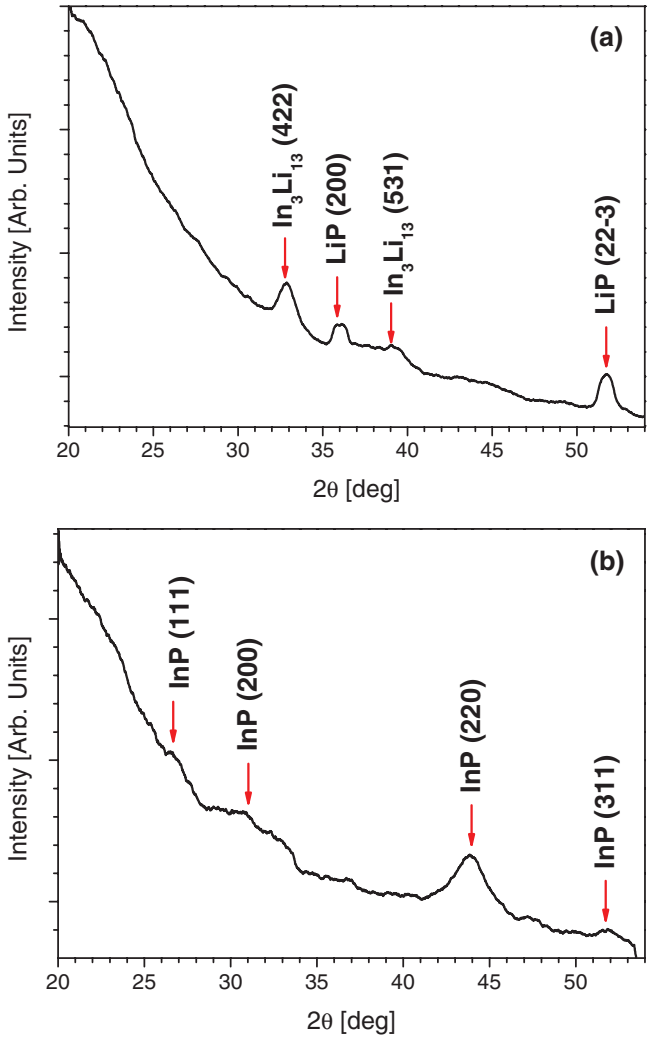

Figure 7. XRD patterns of the InP anode: (a) fully lithiated, and (b) fully delithiated. The phases $Li_{13}In_3$ and LiP are identified in the lithiated state, and InP in the delithiated state.

Even though the fading of the gravimetric capacity amount to about 57% after 13 cycles, the present approach represents a good alternative to the few reported InP anodes,[5,6,13] since the advantages of our approach are the high capacity per area (∼63 mAh/cm^2), which is more than one order of magnitude larger than for typical commercial batteries,[15] and the avoidance of additives, binders, or any other passive materials, which add weight to the anode and thus reduce the gravimetric capacity of the anode. The gravimetric energy density of the presented porous InP anode is 1.36 Wh/g.

Structural characterization by XRD.— Anodes were prepared with a state of full lithiation and full delithiation by applying a constant potential of 0.15 V and 1.85 V, respectively. The process was stopped when the current reached a steady state. The samples were characterized by XRD and SEM. Fig. 7a and 7b show the XRD patterns of the fully lithiated and fully delithiated anodes. In addition a porous anode, which was not exposed to Li, was investigated with XRD as reference, the relevant XRD pattern showing only a very sharp peak attributed to (200) planes. This peak is expected since single-crystalline (100) oriented InP is used for the anode fabrication.

After lithiation, the anode presents four main refraction peaks. None of the four peaks can be assigned to InP in the fully lithiated state indicating that InP is completely converted to Li alloys. They can be identified as In_3Li_{13}[16] and LiP.[17] Two of the four peaks are identical with the ones found by Cui[5] assigned there as In (111) and In (110). But considering the lattice constants of In (a = 0.325 nm and c = 0.495 nm),[18] this assignment to In is probably not correct. Instead, these peaks can be consistently assigned to the In_3Li_{13} phase according to.[16] The two additional peaks in[5] assigned to InLi are not present in our XRD data.

The remaining two peaks can be assigned to LiP in good agreement with Pralong,[19] who also found no evidence for the existence of a Li_3P in the fully lithiated state in the XRD patterns as proposed by Satya Kishore[6] and Cui[5] in their lithiation reactions. Instead a LiP phase is found being also in good agreement with Pralong. The XRD pattern of the lithiated porous InP anode can be consistently interpreted by the following lithiation reaction:

$$3\,InP + 16\,Li^+ + 16\,e^- \rightarrow Li_{13}In_3 + 3\,LiP. \qquad [2]$$

This reaction implicates that about 5.3 Li atoms are stored per molecule in InP, in agreement with the observations of Satya Kishore et al.[6] Nevertheless, there might exist additional lithiated phases, but they could not be identified by XRD analysis. The delithiated sample exhibits diffraction peaks of InP as observed in,[5] evidencing the reversibility of the lithiation. This is a positive aspect of InP, in contrast to other metal phosphides, where the lithiation process is not completely reversible, as is the case for CoP_3 and Sn_4P_3.[20,21] The broadness of the peaks gives an indication of the nanocrystalline nature of InP after delithiation. Additional broad peaks of low intensity could be also observed, but they cannot be unequivocally assigned to any crystalline phases. Nevertheless it is possible that they are remaining Li-P and Li-In phases.

Structural characterization by SEM.— Fig. 8a is a top view on the anode after being charged to 1.85 V. For investigating the anode structure after lithiation, the half-cell was disassembled in a glove box under an Ar-atmosphere. The image shows mostly geometric cracks, preferentially in ⟨110⟩-direction, which is the natural fracture direction for InP. Therefore, it is most probable, that the anode fracturing occurred during disassembling of the half cell and mounting on the sample holder for the SEM investigation. The white fibers on top of the InP membrane are not detached InP pore walls, but originate from the glass fiber microfilter used as separator.

In Fig. 8b the microstructure of the lithiated anode surface is depicted. The almost perfect hexagonal pore arrangement is barely maintained in the fully lithiated state. The pore walls increased enormously in width leaving hardly any visible free space. Nevertheless there are still small areas visible where the pore structure is almost maintained. A magnified view on an area like this is presented in Fig. 8c exhibiting an additional sub-micron texture of the pore walls. In the left part of this image, the pore arrangement before lithiation can be clearly identified, while in neighboring areas this arrangement is lost. The reason for this behavior is the local difference in the pore wall thickness. From this one can conclude that it is possible to compensate the increase in the volume due to the incorporation of Li atoms into the InP crystal structure if the pore walls are thin enough. If the pore walls exceed a certain thickness, the pore walls can fracture at the corners of the pores, as shown in Fig. 8c. A faceting of the pore walls is observed in areas with and without maintained pore arrangement. This faceting is not restricted to the surface, but occurs over the total length of the pore wall as shown in Fig. 8d. A specialty of this faceting is that it exhibits a regular sequence of bulging and necking. This oscillation in the pore wall is self-induced and in anti-phase to neighboring pore walls as depicted in the inset of Fig. 8d. Such anti-phase oscillation can be generally explained by a mechanism combining mutually exerted pressure between neighboring pore walls due to lack of space and a negative feedback for Li transport through the pore walls. Similar anti-phase oscillations have been found, e.g. for the growth of macropores in n-Si.[22] The oscillation in anti-phase is an indication for a periodic recovery of the Li ion concentration in neighboring pores.

In Fig. 9 the porous anode is shown after being charged to 1.85 V and discharged to 0.15 V. This anode is also disassembled in a glove

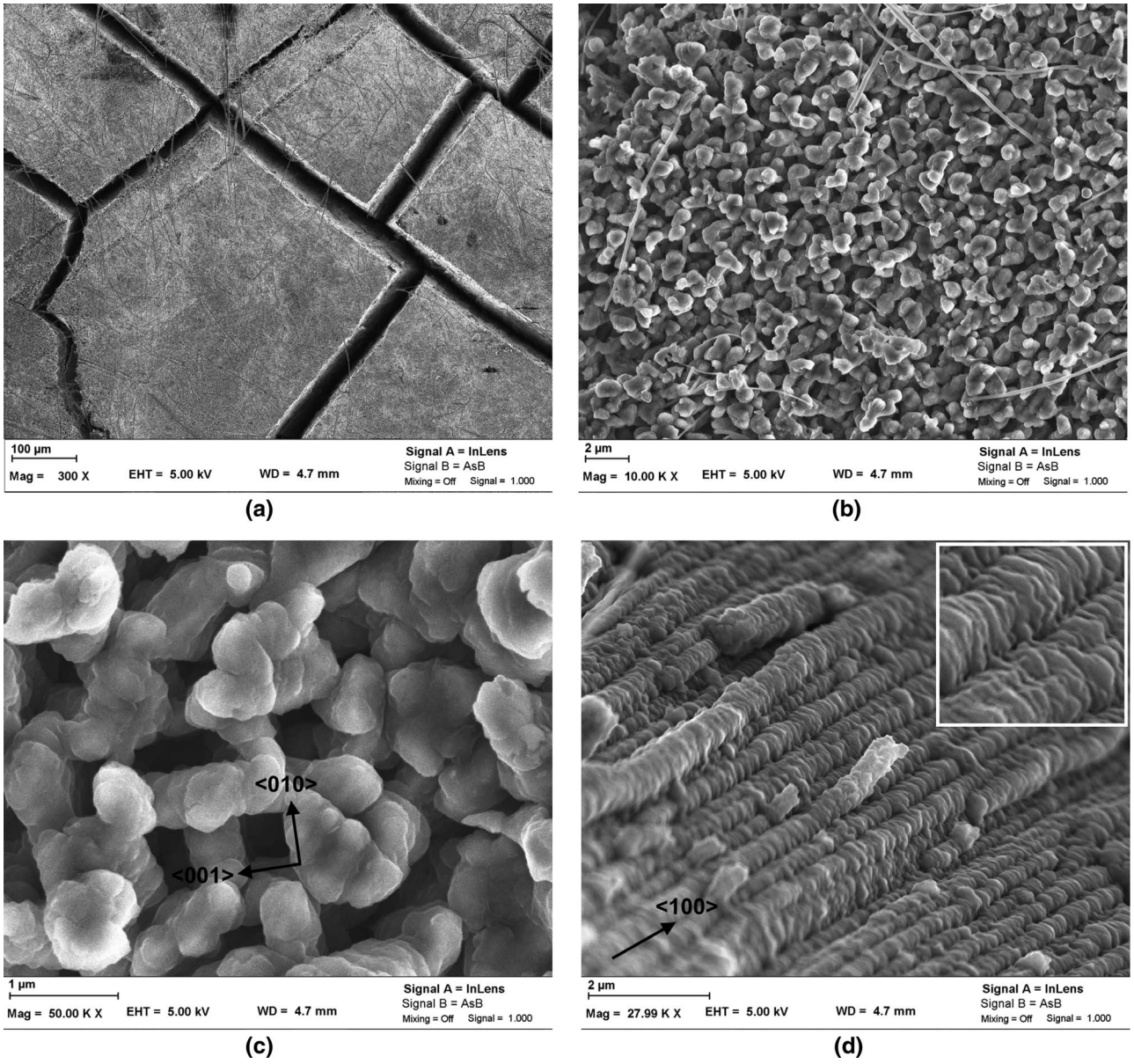

Figure 8. Top view on the fully lithiated porous InP anode showing (a) the macroscopic surface ((100) plane), (b) the microscopic texture ((100) plane), (c) the submicron texture ((100) plane, vectors indicating pore orientation), and (d) the tilted cross-sectional view on the ((110) plane, vectors indicating pore orientation) plane of the InP anode near to the surface, inset: high magnification image of the structure.

box under an Ar-atmosphere before being investigated under the SEM. Fig. 9a is a top view on the surface of the anode. The surface is almost completely covered with the remaining SEI layer, only partially the pore openings (black dimples) and the top parts of pore walls are visible. No blow-outs or big craters are detectable on the surface of the anode indicating the rather good condition of the surface after discharging. The surface-near part of the anode is shown in cross-section in Fig. 9b. Since no delamination or pulverization of pore walls occurred during delithiation, the pore structure is basically maintained. The pore walls are partially covered by the SEI layer. The highly magnified image of Fig. 9b – shown in Fig. 9c – reveals that the anti-phase oscillations in the pore wall thickness due to the lithiation is even maintained after complete discharging of the anode, although the thickness oscillations of the pore walls are far less pronounced compared to the fully lithiated state shown in Fig. 8d. This reduction is thus a direct consequence of discharging the anode. Compared to the pore wall thickness of 160 nm of the non-lithiated anode shown in Fig. 1b, the pore wall thickness of the discharged anode remains highly increased indicating an irreversible structural change of the InP pore walls most probably caused by a permanent incorporation of Li into the crystal structure of InP.

Figure 9d is the cross-sectional image in the middle of the anode. The pore walls also show the oscillations of the pore walls, even though highly reduced compared to the lithiated status, as seen best in the inset of Fig. 9d. The bright particles lying on the pore walls detached from the anode probably during the discharging, since they were not found in the lithiated state, Fig. 8d. As the pore walls do not show a strong thickness oscillation after discharging and the particle size is in the lower nanometer range (see the inset of Fig. 9d), one might speculate that these particles are the result of delaminated facets from the pore walls. Due to the fact that these particles are not electrically connected to the anode anymore, they will not contribute to the capacity on further charging and are a possible reason for the capacity fading observed on further cycling.

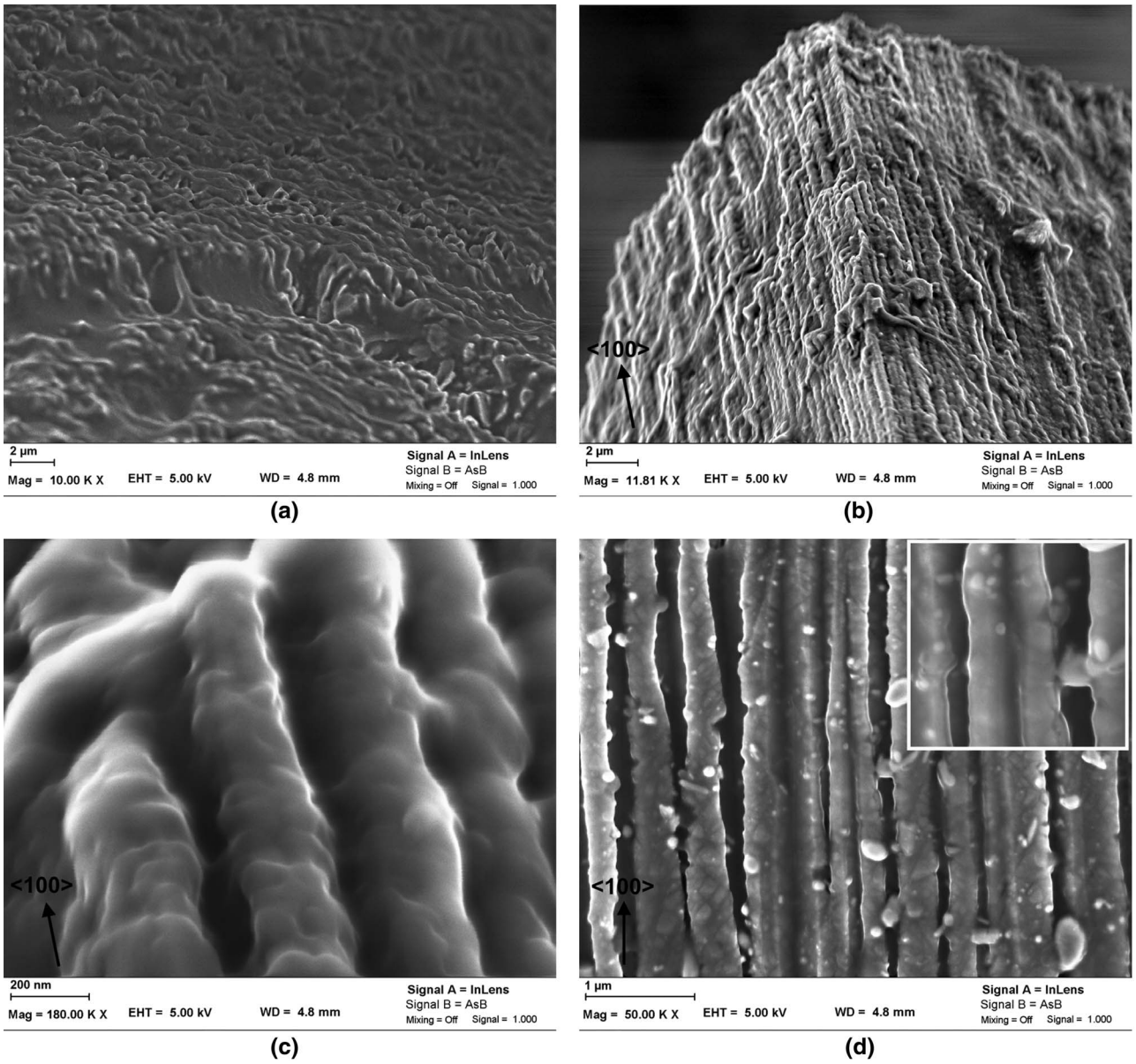

Figure 9. (a) Top view ((100) plane) on the fully delithiated surface of the porous InP anode, (b) cross-sectional view ((110) plane, vectors indicating pore orientation) on the anode surface-near, (c) surface-near in very high magnification ((110) plane, vectors indicating pore orientation) showing the maintained faceting after delithiation, and (d) in the middle of the anode, ((110) plane, vectors indicating pore orientation), inset: high magnification image of the structure.

Conclusions

In this work the complete fabrication of an InP anode for Li-ion batteries is shown. The great advantage of this anode concept is the high capacity per area (∼63 mAh/cm^2). The second advantage is that any additives, binders, or other passive materials, e.g. for mechanical support, such as stainless steel foils, are avoided. The Li alloys found due to lithiation are In_3Li_{13} and LiP. It was found that due to the lithiation an anti-phase oscillation of neighboring pore walls developed that can be explained by means of a mechanism combining mutually exerted pressure between neighboring pore walls due to lack of space and a negative feedback for Li transport through the pore walls. The delithiation of the porous anode results in the formation of nanocrystalline InP showing the reversibility of the lithiation/delithiation process. However the anti-phase oscillations in the pore walls are maintained and no delamination or large-scale pulverization of pore walls was observed indicating that using porous membranes is useful to compensate the volume expansion due to lithiation. Nevertheless, there is much room for improvement of the porous anode performance. In the future the capacity fading of the InP anode during cycling could be improved by decreasing the width of the pore walls in order to further reduce mechanical stress during delithiation. Another strategy could be to coat the pore walls with a thin layer of carbon to improve the formation of the SEI at the InP/electrolyte interface, as shown for Si nanotubes by.[8]

Acknowledgments

This work was funded by the DFG as part of the special research field 855 “magnetoelectric composite materials - biomagnetic interfaces of the future” and by the BMBF through the “AlkaSuSi” project under grant number 03X4618B.

References

1. Y. Lu, J. P. Tu, C.-D. Gu, X.-L. Wang, and S. X. Mao, *J. Mater. Chem.*, **21**, 17988 (2011).
2. C.-M. Park, J.-H. Kim, H. Kim, and H.-J. Sohn, *Chem. Soc. Rev.*, **39**, 3115 (2010).

3. D. Larcher, S. Beattie, M. Morcette, K. Edström, J. C. Jumas, and J. M. Tarascon, *J. Mater. Chem.*, **17**(36), 3759 (2007).
4. C. K. Chan, R. Ruffo, S. S. Hong, and Y. Cui, *J. Power Sources*, **189**, 1132 (2009).
5. Y.-H. Cui, M.-Z. Xue, X.-L. Wang, K. Hu, and Z.-W. Fu, *Electrochem. Commun.*, **11**, 1045 (2009).
6. M. V. V. M. Satya Kishore and U. V. Varadaraju, *J. Power Sources*, **328**, 594 (2006).
7. H. C. Shin, J. A. Corno, J. L. Gole, and M. Liu, *J. Power Sources*, **139**(1-2), 314 (2005).
8. M.-H. Park, M. G. Kim, J. Joo, K. Kim, J. Kim, S. Ahn, Y. Cui, and J. Cho, *Nano Lett.*, **9**(11), 3844 (2009).
9. K. Nishio, S. Tagawa, T. Fukushima, and H. Masuda, *Electrochem. Solid-State Lett.*, **15**(4), A41 (2012).
10. M. Leisner, J. Carstensen, and H. Föll, *Nanoscale Res. Lett.*, **5**(7), 1190 (2010).
11. S. Langa, I. M. Tiginyanu, J. Carstensen, M. Christophersen, and H. Föll, *Electrochem. Solid-State Lett.*, **3**(11), 514 (2000).
12. H. Föll, H. Hartz, E. K. Ossei-Wusu, J. Carstensen, and O. Riemenschneider, *Phys. Stat. Sol. RRL*, **4**(1), 4 (2010).
13. H.-G. Ahn, H.-J. Sohn, and T. Kang, in *Proceedings, 202nd meeting of the electrochemical society*, Salt Lake City, USA (20-24 October 2002).
14. B. Laik, L. Eude, J. P. Pereira-Ramos, C. Sorin Cojocaru, D. Pribat, and E. Rouvière, *Electrochim. Acta*, **53**, 5528 (2008).
15. L-F. Cui, Y. Yang, C.-M. Hsu, and Y. Cui, *Nano Letters*, **9**(9), 3370 (2009).
16. J. Stöhr, W. Müller, and H. Schäfer, *Z. Naturforsch.*, **B 33**, 1434 (1978).
17. W. Honle and H. von Schnering, *Z. Kristallogr.*, **155**, 307 (1981).
18. S. S. Oh, D. H. Kim, M. W. Moon, A. Vaziri, M. Kim, E. Yoon, K. H. Oh, and J. W. Hutchinson, *Adv. Mater.*, **20**, 1093 (2008).
19. V. Pralong, D. C. S. Souza, K. T. Leung, and L. F. Nazar, *Electrochem. Commun.*, **4**, 516 (2002).
20. R. Alcàntara, J. L. Tirado, J. C. Jumas, L. Monconduit, and J. Olivier-Fourcade, *J. Power Sources*, **109**, 308 (2002).
21. B. Leòn, J. I. Corredor, J. L. Tirado, and C. Pèrez-Vicentez, *J. Electrochem. Soc.*, **153**, A1829 (2006).
22. A. Cojocaru, J. Carstensen, M. Leisner, H. Föll, and I. M. Tiginyanu, *Phys. Stat. Sol. (c)*, **206**(7), 1533 (2009).